Arecibo Timing and Single Pulse Observations of 18 Pulsars

Wojciech Lewandowski

Toruń Centre for Astronomy, Nicolaus Copernicus University, Gagarina 11, 87-100 Toruń, Poland

Alex Wolszczan

Department of Astronomy and Astrophysics, The Pennsylvania State University, 525 Davey Laboratory, University Park, PA 16802, USA

Toruń Centre for Astronomy, Nicolaus Copernicus University, Gagarina 11, 87-100 Toruń, Poland

Grażyna Feiler

Toruń Centre for Astronomy, Nicolaus Copernicus University, Gagarina 11, 87-100 Toruń, Poland

Maciej Konacki

Nicolaus Copernicus Astronomical Center, Polish Academy of Sciences, Rabia nska 8, 87-100 Toruń, Poland

Department of Geological and Planetary Sciences, California Institute for Technology, MS 150-21, Pasadena, CA 91125, USA

Tomasz Sołtysiński

Institute of Physics, Szczecin University, Wielkopolska 15, 70-451 Szczecin, Poland

ABSTRACT

We present new results of timing and single pulse measurements for 18 radio pulsars discovered in 1993 - 1997 by the Penn State/NRL declination-strip survey conducted with the 305-m Arecibo telescope at 430 MHz. Long-term timing measurements have led to significant improvements of the rotational and the astrometric parameters of these sources, including the millisecond pulsar, PSR J1709+2313, and the pulsar located within the supernova remnant S147, PSR J0538+2817. Single pulse studies of the brightest objects in the sample have revealed an unusual "bursting" pulsar, PSR J1752+2359, two new drifting

subpulse pulsars, PSR J1649+2533 and PSR J2155+2813, and another example of a pulsar with profile mode changes, PSR J1746+2540. PSR J1752+2359 is characterized by bursts of emission, which appear once every 3-5 min. and decay exponentially on a ∼45 sec timescale. PSR J1649+2533 spends ∼30% of the time in a null state with no detectable radio emission.

Subject headings: pulsars - general, astrometry, pulsars - specific: PSR J0538+2817, PSR J1649+2533, PSR J1709+2313, PSR J1746+2540, PSR J2155+2813

1. Introduction

Most of the large-scale, undirected pulsar surveys conducted since the time of discovery of the millisecond pulsars (Backer et al. 1982) have been driven by an astrophysically well motivated desire to detect more of these rapidly rotating neutron stars (e.g. Phinney & Kulkarni 1994; Lorimer 2001). This is certainly true for the spectacularly successful southern hemisphere surveys with the Parkes 64-m telescope (Manchester et al. 2001; Edwards & Bailes 2001), as well as for a number of less extensive, but more sensitive Arecibo surveys that have contributed several milestone pulsar discoveries (Camilo 1995). In fact, the progress in this field has become particularly dramatic after the first discoveries of millisecond pulsars away from the galactic plane (Wolszczan 1991), which indicated an approximately isotropic distribution of these objects in the solar neighborhood.

Along with the millisecond pulsars, the surveys usually discover the objects of the so-called slow pulsar variety in much greater numbers. For example, the Arecibo drift-scan searches carried out since 1991 have found 9 millisecond pulsars and at least 70 slow pulsars (Foster et al. 1995; Camilo et al. 1996; Ray et al. 1996; Xilouris et al. 2000; McLaughlin, Cordes & Arzoumanian 2000; Lommen et al. 2000; Lorimer et al. 2002; Chandler 2003). Newly discovered slow pulsars certainly deserve to be subjected to close scrutiny. For example, there exists a possibility that some slow pulsars have black hole or planetary companions (e.g. Thorsett & Dewey 1993; Lipunov et al. 1994; Kalogera et al. 2001). Furthermore, timing measurements of pulsars, especially the younger ones, remain the only source of experimental evidence concerning the neutron star seismology (see Cheng et al. 1988). Finally, there is also an open issue of the pulsar emission mechanism (Melrose 2000), whose final clarification may require new, possibly unanticipated kinds of evidence.

The Penn State/NRL survey (Foster et al. 1995) and the subsequent untargeted observations by the Penn State group throughout the Arecibo upgrade period have effectively covered about 850 square degrees of the sky in a manner dictated by the logistics of the

telescope scheduling. They have contributed 3 new millisecond pulsars and 16 slow ones to the total number of the drift-scan survey discoveries quoted above. The millisecond pulsars PSR J1640+2224 and PSR J1713+0747 have been systematically monitored at Arecibo since the time of their discovery. The timing models for these objects have been published by Wolszczan et al. (2000) and Camilo, Foster and Wolszczan (1994), respectively. Our continuing observations discussed in this paper have established an accurate timing model for the third millisecond pulsar, PSR J1709+2313, positively verified two of the four unconfirmed slow pulsar candidates included in Foster et al. (1995), PSR J2151+2315 and PSR 2155+2813, and discovered two additional slow pulsars, PSR 1813+1822 and PSR J1908+2351. Two of our seemingly original discoveries, PSR J1549+21 and PSR J1906+16, have proven to be pulsars detected by other searches (Lorimer, private communication; Camilo 1995). Finally, the slow pulsar candidates, PSR B1840+13 and PSR B2208+18, and the millisecond pulsar candidate, PSR B1735+13, have not been confirmed.

In this paper, we present refined timing models for the millisecond pulsar PSR J1709+23, the pulsar PSR J0538+2817 in the supernova remnant S147, and the sixteen confirmed slow pulsars discovered by the Penn State/NRL surveys since 1991. The model for PSR J1709+2313 includes a significant proper motion measurement. For all pulsars listed in Foster et al. (1995), both the spin parameters and the timing positions have been significantly improved. Timing parameters for the two new slow pulsars are published here for the first time. We also present the results of single pulse observations of the brightest objects in the sample. These include the unusual "bursting" pulsar, PSR J1752+2359, two new drifting subpulse pulsars, PSR J1649+2533 and PSR J2155+2813, and a new mode changing pulsar, PSR J1746+2540.

Our observations and data analysis are described in Section 2. In Section 3, we give the details of the new timing models for the millisecond pulsar PSR J1709+2313, PSR J0538+2817, the pulsar located inside the supernova remnant S147, and for the 16 slow pulsars. Section 4 is devoted to the single pulse analysis of three pulsars from this sample and our conclusions are given in Section 5.

2. Observations and Data Analysis

The pulse timing and the single pulse observations discussed in this paper have been made with the 305-m Arecibo radiotelescope using the dual-circular polarization receiving systems at 430 MHz and 1400 MHz and the Penn State Pulsar Machine (PSPM). Timing observations made at Arecibo before 1995 with the 40 MHz correlation spectrometer as a pulsar backend are discussed in Foster et al. (1995) and Cadwell (1997).

The PSPM pulsar backend is a 2 × 128 × 60 kHz, computer controlled processor designed to conduct fast sampled pulsar searches and precision timing measurements. Technical details of the backend are given in Cadwell (1997). In the timing mode, the dual-polarization, left- and right-circularly polarized signals were added together, smoothed with appropriate time constants ranging from 32 μs to 700 μs, 4-bit quantized, and averaged synchronously with the Doppler-shifted pulsar period. The average pulse profiles, with the number of phase bins chosen to ensure an approximately one milliperiod time resolution, were time-tagged using the observatory's hydrogen-maser clock and stored for further analysis. A typical integration time for each profile was 180 s. For the purpose of single pulse analysis, the data were taken in the search mode by continuously sampling the polarization summed signal at 80 μs intervals using a 100 μs post-detection time constant. In this case, the phasing of the single pulses was accomplished in the off-line analysis.

The topocentric times-of-arrival (TOA) of pulses were calculated by cross-correlating the average pulses with high signal-to-noise template profiles. For each pulsar, the standard timing analysis package TEMPO (http://www.pulsar.princeton.edu/) was then employed to convert the TOAs to the solar system barycenter using the JPL DE200 ephemeris (Standish, 1990) and to perform least-squares fits of appropriate timing models to the data. In the case of slow pulsars, the models included the pulsar rotation period P and its slowdown rate $\dot{P}$, celestial coordinates α_{J2000} and δ_{J2000}, and the dispersion measure DM. For PSR J1709+2313, the additional model parameters were the pulsar's proper motion and the five Keplerian elements of its binary orbit. The proper motion was also included in the timing model for PSR J0538+2817, in which case the fitting of astrometric parameters was carried out in ecliptic coordinates, because of the pulsar's proximity to the ecliptic plane (see also Kramer et al. 2003).

3. Timing Models and Other Parameters for Individual Sources

The timing results for two of the 18 pulsars presented in this paper, PSR J1709+2313 and PSR J0538+2817, are discussed separately in this Section, because of their respective memberships of the millisecond pulsar population and the group of young pulsars associated with supernova remnants. A joint discussion is presented for the remaining sources, for which the basic timing model was sufficient to describe their properties.

The pulse widths and flux densities of the 18 pulsars were measured following the procedures described by Camilo and Nice (1995) and Lorimer, Camilo and Xilouris (2002). The widths listed in Tables 1-3 are given as the equivalent width w_e (the width of a top-hat pulse, having the same area and height as the profile), w_{50}, and w_{10} measured at the 50%,

and 10% intensity level, respectively. Finally, the timing data were used to compute the most important derived pulsar parameters (Table 4): the distance estimate, d, obtained from the Taylor and Cordes (1993) model of the Galactic electron density distribution; height above the Galactic plane, z=d sin b; pulsar luminosity at 430 MHz, L_{430}=$S_{430}d^2$; spin-down age, τ=$P/2\dot{P}$; spin-down energy-loss rate, $\dot{E}$=$4\pi^2 I\dot{P}/P^3$ (the moment of inertia I=10^{45} g cm^2); and dipole magnetic field, B=$3.2\times10^{19}(P\dot{P})^{1/2}$ G. Uncertainties of the parameters that involve the pulsar distance depend on the corresponding errors in distance estimates derived from the Taylor & Cordes (1993) model and may be as large as 30%.

3.1. The Millisecond Pulsar PSR J1709+2313

The 4.6-ms pulsar PSR J1709+2313 was discovered in June 1994, during the final months before the upgrade related shutdown of the Arecibo telescope. The initial timing model for this faint binary millisecond pulsars has been published by Foster et al. (1995). Because of the insufficient data, the model could not be significantly improved until after the reopening of the telescope in late 1997 (Cadwell 1997).

New observations conducted in 1997-2003 involved systematic TOA measurements at 430 MHz. Only a few successful 1400 MHz observations were made, due to the pulsar's faintness at frequencies above 1 GHz. The average pulse profiles of PSR J1709+2313 at the two frequencies (Fig. 1a) are quite similar and exhibit at least three broad components and an interpulse. The two frequency observations were essential in obtaining an accurate DM measurement of the pulsar. They were also used to estimate the pulsar's flux density (Table 1) and the corresponding spectral index between 430 MHz and 1400 MHz. Because the 1400 MHz flux was measurable during the infrequent episodes of interstellar scintillation maxima of the pulsar, only an upper limit to the spectral index, $\alpha << -2$, could be derived. In fact, its real value is likely to be among the steepest spectral indices measured for the millisecond pulsars (e.g. Kramer et al. 1998).

The best-fit residuals for the timing model assuming a 22.7-day, low-eccentricity binary orbit of the pulsar are shown in Fig. 1b. With the new TOA measurements of PSR J1709+2313, it was possible to obtain a phase-connected timing solution that spans the entire 1994-2003 observing period and includes a significant proper motion measurement (Table 1). Because the pulsar is weak and has a broad pulse profile, the rms residual for the best-fit model is relatively large and amounts to 20 μs for 180-s integrations or 5.5 μs for daily-averaged TOAs.

The very small $\dot{P}$ of PSR J1709+2313 (Table 1) makes it necessary to correct its value

for kinematic biases related to acceleration due to proper motion (Shklovskii 1970), and to vertical and differential accelerations in the Galaxy (Damour & Taylor 1991). Following these authors, a total kinematic correction to $\dot{P}$ takes the form:

$$\left(\frac{\dot{P}}{P}\right)^k = -\frac{a_z \sin b}{c} - \frac{v_0^2}{cR_0}\left[\cos l + \frac{\beta}{\sin^2 l + \beta^2}\right] + \mu^2 \frac{d}{c}, \quad (1)$$

where a_z is the vertical component of Galactic acceleration, which can be calculated from a model of the Galactic potential published by Kuijken & Gilmore (1989), l and b are the pulsar's galactic coordinates, μ is its proper motion, c is the speed of light, R_0 and v_0 denote the galactocentric radius and galactic circular velocity of the Sun, respectively, and $\beta \equiv d/R_0 - \cos l$. For PSR J1709+2313, all the three terms in equation (1) are significant and yield a total kinematic correction, $\dot{P}_k$, listed in Table 1. The error in $\dot{P}_k$ is dominated by a $\sim$30% uncertainty of the pulsar distance estimate. The derived parameters of the pulsar given in Table 4 have been calculated with the corrected value of $\dot{P}$.

3.2. PSR J0538+2817 in the Supernova Remnant S147

PSR J0538+2817, discovered by Anderson et al. (1996), is located within the well-known supernova remnant S147 (G180.0−1.7). Based on the positional coincidence and a reasonable similarity of the estimated distances and ages of the two objects, these authors have hypothesized that the pulsar could be physically related to the remnant. Initial Arecibo timing observations of PSR J0538+2817 discussed by Anderson et al. (1996) were carried out in 1994 and they were continued with the Effelsberg and Jodrell Bank telescopes by Kramer et al. (2003).

We have resumed timing observations of PSR J0538+2817 with the PSPM after the Arecibo upgrade and collected TOA measurements at 430 MHz and 1400 MHz over a 2.5-yr period beginning in late 1998. The average pulse profiles of the pulsar have been published by Anderson et al. (1996). Good quality flux density measurements of PSR J0538+2817 at the two frequencies (Table 2) were used to calculate its spectral index $\alpha = -1.2 \pm 0.1$. This value is the same as the index derived by Maron et al. (2000) from the flux density measurements at 1.4 GHz and 4.9 GHz and it implies that the emission of this pulsar over the 0.43 GHz - 4.9 GHz frequency range is adequately described by a simple power-law spectrum.

A timing model including the pulsar's spin and astrometric parameters and the dispersion measure was fitted to data in two steps. First, the two frequency TOA measurements were used to determine DM variations over the observing period. To accomplish this, the

DM was averaged over five partially overlapping, 3-6 month intervals between 1999 and 2002. As illustrated in Fig. 2a, the DM of PSR J0538+2817 shows an approximately monotonic increase at a rate of $\sim$0.008 pc cm^{-3}/yr. Second, with the DM variations fixed, the remaining parameters were determined from a least-squares fit of the model to the TOA measurements. Slow TOA variations caused by the timing noise were fitted out by including a second time derivative of the pulsar's spin period in the model. Because of a relatively short, 2.5-yr span of the data used in this analysis, we found it unnecessary to model the timing noise by means of more precise methods (e.g. Hobbs, Lyne & Kramer 2003). The resulting best-fit TOA residuals are shown in Fig. 2b and the final model parameters are listed in Table 2. The fit is characterized by an rms residual of 169 μs (111 μs for daily-averaged TOAs). Other pulsar parameters derived from the timing model are given in Table 4.

3.3. Results for the 16 Slow Pulsars

Approximate timing models for 12 out of the 16 "ordinary", slow pulsars discussed here have been published by Foster et al. (1995) along with the list of unconfirmed pulsar candidates. Our timing observations initiated after the Arecibo upgrade have resulted in significant improvements of these models and in establishing the models for two more confirmed pulsars from the original list, PSR J2151+2315 and PSR J2155+2813. In addition, sufficient data have been gathered for two more recently discovered pulsars, PSR J1813+1822 and PSR J1908+2351, to determine their timing behavior for the first time.

All the post-upgrade timing observations of the 16 pulsars were conducted at 430 MHz between late 1998 and mid-2001. For pulsars observed before 1995, the new TOAs were phased with the old ones across the 3-yr Arecibo upgrade gap in the model fitting process. For the four newer objects mentioned above, the TOA modeling was based on the data collected over a 2.5-yr post-upgrade period. The least-squares fits of the timing models included the standard spin and astrometric parameters of the pulsars. Because no second frequency data were available for these objects, their dispersion measures were determined by splitting the 8 MHz bandpass of the PSPM into two bands, 4 MHz apart, calculating the TOAs for the two center frequencies and fitting for DM using the two-frequency TOA sets. The best-fit timing and derived parameters for all the 16 pulsars are listed in Tables 3 and 4, respectively. Typically, the models fitted have rms residuals in the 0.5 - 1.5 ms range for a 180 s integration time per TOA measurement, depending on the pulse strength and width.

The average pulse profiles of 12 pulsars discovered before 1995 have been published by Foster et al. (1995). The profiles of the four newer pulsars discussed above are shown in Fig. 3. Also shown are the two profiles of PSR J1746+2540 which was found to undergo

clearly distinguishable profile mode changes. In addition, we display in Fig. 3 an improved profile for PSR J1938+0650, whose shape originally published by Foster et al. (1995) was artificially broadened, because of the incorrect timing model used in the pulse averaging process.

4. Single Pulse Behavior of Three Pulsars

The purpose of the single pulse analysis was to search the data for possible presence of phenomena such as subpulse drifting, nulling or pulse mode changes. To accomplish this, blocks of 1024 to 4096 consecutive single pulses were phased up using the ephemerides derived from the up-to-date pulse timing models and displayed as pulse phase vs. pulse number diagrams for visual inspection and further analysis.

4.1. Drifting Subpulses in PSR J1649+2533 and PSR J2155+2813

Drifting subpulses represent an organized behavior of the emission peaks within the average pulse envelope which manifests itself as a correlated progression of the subpulse phase over consecutive pulse periods (e.g. Backer 1973). Another phenomenon, more common in older pulsars, is the pulse nulling - a sudden cessation of the pulsed emission followed by an equally sudden emission onset several periods later (e.g. Ritchings 1976, Biggs 1992).

We have identified the drifting subpulses in PSR J1649+2533 and PSR J2155+2813. Because the drift rate is high in both pulsars and cannot be easily detected in the raw single pulse data, the corresponding drift patterns are presented in Fig. 4 in the form of two-dimensional autocorrelation functions of the pulse intensity distribution in the pulse number/pulse phase plane. These plots clearly reveal the presence of periodic patterns of a rapidly drifting emission in both pulsars.

The subpulse drift patterns are usually parametrized in terms of the subpulse separation, P_2, and the spacing between the adjacent subpulse bands, P_3 (e.g. Backer 1973). The measured values of these parameters for PSR J1649+2533 and PSR J2155+2813 are 19.8 ms and 15.7 ms for P_2, and $2.2P$ and $2.5P$ for P_3, respectively. In addition to subpulse drifting, PSR J1649+2533 exhibits the pulse nulling, which occurs approximately 30% of the time (Fig. 5a).

4.2. Burst-like Emission of PSR J1752+2359

This pulsar has been selected for additional observations because of its unusually long nulling periods. After the initial, post-discovery study by Cadwell (1997), we have observed it on several occasions between 2000 and 2002. As shown in Fig. 5b, the pulsar spends 70-80% of the time in a "quasi-null" state. The "on-states" occur once every 400-600 periods and last, on average, for ∼100 periods. A more detailed inspection of the on-states (Fig. 5c) reveals that these burst-like emissions are quite similar in shape and duration and they decay into a null state in a manner that is quite reasonably described by a $te^{-t/\tau}$ function with τ ∼45 seconds.

A comparison of the single pulse characteristics of PSR J1752+2359 with a more typical nulling behavior of PSR J1649+2533 (Fig. 5a) clearly shows that the two phenomena exhibit distinctly different morphologies, because PSR J1752+2359 switches off gradually, rather than suddenly, as observed in the nulling pulsars (Ritchings 1976, Deich et al. 1986, Biggs 1992). Moreover, the astonishing morphological similarity of the individual on-states and their very similar timescales and repetition rates are unique among the nulling pulsars. To our knowledge, these emission characteristics of PSR J1752+2359 make it an exceptional member of the pulsar population.

5. Discussion

The pulsars discussed in this paper fall into three evolutionary categories as indicated in the P-$\dot{P}$ diagram shown in Fig. 6. When interpreted in terms of the rotating magnetic dipole model (Pacini 1968; Gold 1968), the location of a pulsar in this diagram depends on the strength of its surface magnetic field ($\sim (P\dot{P})^{1/2}$) and on its characteristic age ($\tau = P/2\dot{P}$). Within this framework, the relatively young pulsar PSR J0538+2817, possibly still associated with the supernova remnant S147, appears close to the cluster of similarly young objects, whereas the 16 "normal" pulsars fall in the area that is occupied by the largest, intermediate age category. The two possible exceptions in this group are PSR J1813+1822 and PSR J1908+2351 (Table 4), which have characteristic ages well above 100 Myr, magnetic fields below 10^{11} Gauss, and may more properly be categorized as mildly "recycled" pulsars which originated from disrupted binaries (e.g. Bailes 1989). Finally, as expected, the millisecond pulsar PSR J1709+2313 is found among other members of the old, recycled pulsar population (Phinney & Kulkarni 1994).

5.1. PSR J1709+2313

The timing model of PSR J1709+2313 presented here replaces a provisional set of parameters derived from initial observations of the pulsar conducted just before the Arecibo upgrade (Foster et al. 1995). Timing parameters of the pulsar and the resulting old characteristic age, low companion mass, and weak surface magnetic field (Table 1), place this object in the class of low-mass binary millisecond pulsars (LMBPs), presumably orbited by He white dwarf companions (Phinney & Kulkarni 1994). The pulsar's ∼90 km s^{-1} transverse velocity (Table 1) is quite typical for the LMBP population (see Cordes & Chernoff, 1997).

A common explanation for the unrealistically old spindown age of the pulsar is that it must have been born with a spin period close to its observed value (e.g. Camilo, Thorsett & Kulkarni 1994; Nice & Taylor 1995). Assuming that the observed, kinematically corrected spindown, $\dot{P}_i$, is entirely driven by a magnetic dipole radiation, and requiring that the pulsar cannot be older than the estimated age of the Galaxy ($\sim 10 \times 10^9$ yr; Winget et al. 1987), one can estimate the initial spin period, P_0, from the equation:

$$\tau = \frac{P}{2\dot{P}_i}\left[1 - \left(\frac{P_0}{P}\right)^2\right], \tag{2}$$

which reduces to its simpler, more frequently used form, when $P_0 \ll P$. In the case of PSR J1709+2313, equation (2) yields $P_0 \geq$4.1 ms indicating very little period evolution for this pulsar.

Another interesting feature of PSR J1709+2313 is its 22.7-day orbital period, which falls in the "period gap" invoked in the context of modeling of the paths of binary evolution that may lead up to formation of the LMBPs (Camilo 1995). Another such case, PSR J1618-39 with a 22.8-day binary period, has been detected by Edwards and Bailes (2001). As remarked by these authors, the existence of the two objects does weaken the period gap case, but it still does not remove a possibility of underpopulation of the orbital period range between 12 days and 56 days.

5.2. PSR J0538+2817

PSR J0538+2817 in the supernova remnant S147 has been recently studied by Kramer et al. (2003). These authors have used a proper motion measurement of the pulsar, based on timing observations with the Jodrell Bank and the Effelsberg telescopes, to conclude that the object moves away from the center of the remnant at ∼385 km s^{-1}. This result implies that the pulsar's characteristic age of ∼0.6 Myr dramatically overestimates its true age, which

now appears to be close to 30 kyr, and that the pulsar had to be born with the initial spin period not much shorter than the observed one.

The Arecibo timing parameters of PSR J0538+2813 (Table 2) agree with those obtained by Kramer et al. (2003) within the measurement errors. Although the significance of our proper motion estimate for the pulsar is low, because of the short, 2.5-yr span of observations, both the magnitudes and signs of this effect in the ecliptic coordinates are in a reasonable agreement with the values published by Kramer et al. Therefore, we conclude that, within the precision limits imposed by the extent of the Arecibo timing data, they are consistent with the results presented by these authors in favor of the actual association of PSR J0538+2813 with S147.

5.3. PSR J1649+2533, PSR J1752+2359, and PSR J2155+2813

The slow pulsars, PSR J1649+2533 and PSR J2155+2813 belong to the slowly growing group of relatively rare objects characterized by drifting subpulses, nulling and, in some cases, a combination of both (see Ord, Edwards & Bailes 2001, Lorimer, Camilo & Xilouris 2002, Chandler 2003, and Edwards & Stappers 2003, for the description of other recent detections). Studies of these phenomena have been regarded as very important for our understanding of the detailed physics of pulsar emission (e.g. Ruderman & Sutherland 1975, Biggs 1992, Deshpande & Rankin 1999). This appears to be particularly true for analyses of the interaction between subpulse drifting and nulling (Lyne & Ashworth 1983, Deich et al. 1986, Vivekanand & Joshi 1997, van Leeuwen et al. 2003). As no unified picture of this interaction has emerged so far, possibly because of the insufficient statistics, new pulsars like PSR J1649+2533, displaying both drifting and nulling, are obvious candidates for further, more detailed observations.

The spin characteristics of the bursting pulsar, PSR J1752+2359 make it a fairly typical member of the slow pulsar population (Table 3, Fig. 6). In addition, the timing and the pulse profile morphology data do not indicate any pulse arrival time and/or pulse shape variability that might be due to orbital motion or precessional beam wobble and could be used to interpret the observed exponentially decaying bursts of emission from the pulsar (Fig. 5b,c). As the pulsar's unusual properties may provide new, useful constraints on the emission process, it is important to observe it at multiple frequencies, including polarization measurements, to achieve a possibly complete phenomenological description of its radio signal before attempting any generalizing conclusions. It may also be interesting to explore an intriguing possibility that PSR J1752+2359 may be a member of a sizeable group of pulsars of the same type that have remained undiscovered because of the very low duty

cycle, burst-like behavior of such objects.

WL, MK, GF and AW were partially supported from the KBN grant 2.P03D.006.16. AW and WL acknowledge partial support from the NSF grant AST-9988217. The authors thank B. Cadwell and R. Foster for their contributions to the early phases of this research. The Arecibo observatory is part of the National Astronomy and Ionosphere center, which is operated by Cornell University under a cooperative agreement with the National Science Foundation.

REFERENCES

Anderson, S. B., Cadwell, B. J., Jacoby, B. A., Wolszczan, A., Foster, R. S. & Kramer, M. 1996, ApJ, 468, 55

Backer, D. C 1973, ApJ, 182, 245

Backer, D. C., Kulkarni, S. R., Heiles, C., Davis, M. M. & Goss, W. M. 1982, Nature, 300, 615

Bailes, M. 1989, ApJ, 342, 917

Biggs, J. D. 1992, ApJ, 394, 574

Cadwell, B. 1997, PhD Thesis, Pennsylvania State University

Camilo, F., Foster, R. S. & Wolszczan, A. 1994, ApJ, 437, L39

Camilo, F. 1995 , in The Lives of the Neutron Stars, Alpar, M. A., Kiziloglu, U., van Paradijs, J. (eds) (NATO ASI Series C, 515; Dordrecht: Kluwer), 243

Camilo, F., Nice, D. J. 1995, ApJ, 445, 756

Camilo, F., Nice, D. J., Shrauner, J. A., Taylor & J. H. 1996, ApJ, 469, 819

Chandler, A. 2003, PhD Thesis, California Institute of Technology

Cheng, K. S., Pines, D., Alpar, M. A. & Shaham, J. 1988, ApJ, 330, 835

Cordes, J. M. & Chernoff, D.F. 1997, ApJ, 482, 971

Damour, T. & Taylor, J. H. 1991, ApJ, 366, 501

Deich, W. T. S., Cordes, J. M., Hankins, T. H. & Rankin, J. M. 1986, ApJ, 300, 540

Deshpande, A. A. & Rankin, J. M. 1999, ApJ, 524, 1008

Edwards, R. T., Bailes, M. 2001, ApJ, 553, 801

Edwards, R. T. & Stappers, B. W. 2003, A&A, 407, 273

Foster, R. S., Cadwell, B. J., Wolszczan, A. & Anderson, S. B. 1995, ApJ, 454, 826

Gold, T. 1968, Nature, 218, 731

Hobbs, G., Lyne, A. G. & Kramer, M. 2003, to appear in proceedings of the conference "Radio Pulsars" held in Chania, Crete, Sept 2002

Kalogera, V., Narayan, R., Spergel, D. N. & Taylor, J. H. 2001, ApJ, 556, 340

Kramer, M., Xilouris, K. M., Lorimer, D. R., Doroshenko, O., Jessner, A., Wielebinski, R., Wolszczan, A. & Camilo, F. 1998, ApJ, 501, 270

Kramer, M., Lyne, A. G., Hobbs, G., Löhmer, O., Jordan, C. & Wolszczan, A. 2003, submitted to ApJL

kuijken, K. & Gilmore, G. 1989, MNRAS, 239, 605

van Leeuwen, A. G. J., Stappers, B. W., Ramachandran, R. & Rankin, J. M. 2003, A&A, 399, 223

Lipunov, V. M., Postnov, K. A., Prokhorov, M. E., Osminkin, E. Yu. 1994, ApJ, 423, L121

Lommen, A. N., Zepka, A., Backer, D. C., McLaughlin, M., Cordes, J. M., Arzoumanian, Z. & Xilouris, K. 2000, ApJ, 545, 1007

Lorimer, D. R. 2001, Living Reviews in Relativity, vol. 4, art. 5

Lorimer, D. R., Camilo, F. & Xilouris, K. M. 2002, AJ, 123, 1750

Lyne, A. G. & Ashworth, M. 1983, MNRAS, 204, 519

Manchester, R. N., Lyne, A. G., Camilo, F., Bell, J. F., Kaspi, V. M., D'Amico, N., McKay, N. P. F., Crawford, F., Stairs, I. H., Possenti, A., Kramer, M. & Sheppard, D. C. 2001, MNRAS, 328, 17

Maron, O., Kijak, J., Kramer, M. & Wielebinski, R. 2000, A&ASup., 147, 195

McLaughlin, M. A., Cordes, J. M., Arzoumanian, Z. 2000, in *IAU Coll. 177, Pulsar Astronomy - 2000 and Beyond, Kramer, M., Wex, N. & Wielebinski, R. (eds) (San Fransisco: ASP)*, 41

Melrose, D. B. 2000, in *IAU Coll. 177, Pulsar Astronomy - 2000 and Beyond, Kramer, M., Wex, N. & Wielebinski, R. (eds) (San Fransisco: ASP)*, 721

Ord, S. M., Edwards, R. & Bailes, M. 2001, MNRAS, 328, 911

Pacini, F. 1967, Nature, 219, 145

Phinney, E. S. & Kulkarni, S. R. 1994, ARA&A, 32, 591

Ray, P. S., Thorsett, S. E., Jenet, F. A., van Kerkwijk, M. H., Kulkarni, S. R., Prince, T. A., Sandhu, J. S. & Nice, D. J., ApJ, 470, 1103

Ritchings, R. T. 1976, MNRAS, 176, 249

Ruderman, M. A. & Sutherland, P. G. ApJ, 196, 51

Shklovskii, I. S. 1970, Soviet Astron., 13, 562

Standish, E. M. Jr. 1990, A&A, 233, 252

Taylor, J. H. & Cordes, J. M. 1993, ApJ, 411, 674

Thorsett, S. E., Dewey, R. J. 1993, ApJ, 419, 65

Vivekanand, M. & Joshi, B. C. 1997, ApJ, 477, 431

Winget, D. E., Hansen, C. J., Liebert, J., van Horn, H. M., Fontaine, G., Nather, R. E., Kepler, S. O. & Lamb, D. Q. 1987, ApJ, 315, L77

Wolszczan, A. 1991, BAAS, 23, 834

Wolszczan, A., Doroshenko, O., Konacki, M., Kramer, M., Jessner, A., Wielebinski, R., Camilo, F., Nice, D. J., & Taylor, J. H. 2000, ApJ, 528, 907

Xilouris, K. M., Fruchter, A., Lorimer, D. R., Eder, J. & Vazquez, A. 2000, in *IAU Coll. 177, Pulsar Astronomy - 2000 and Beyond, Kramer, M., Wex, N. & Wielebinski, R. (eds) (San Fransisco: ASP)*, 21

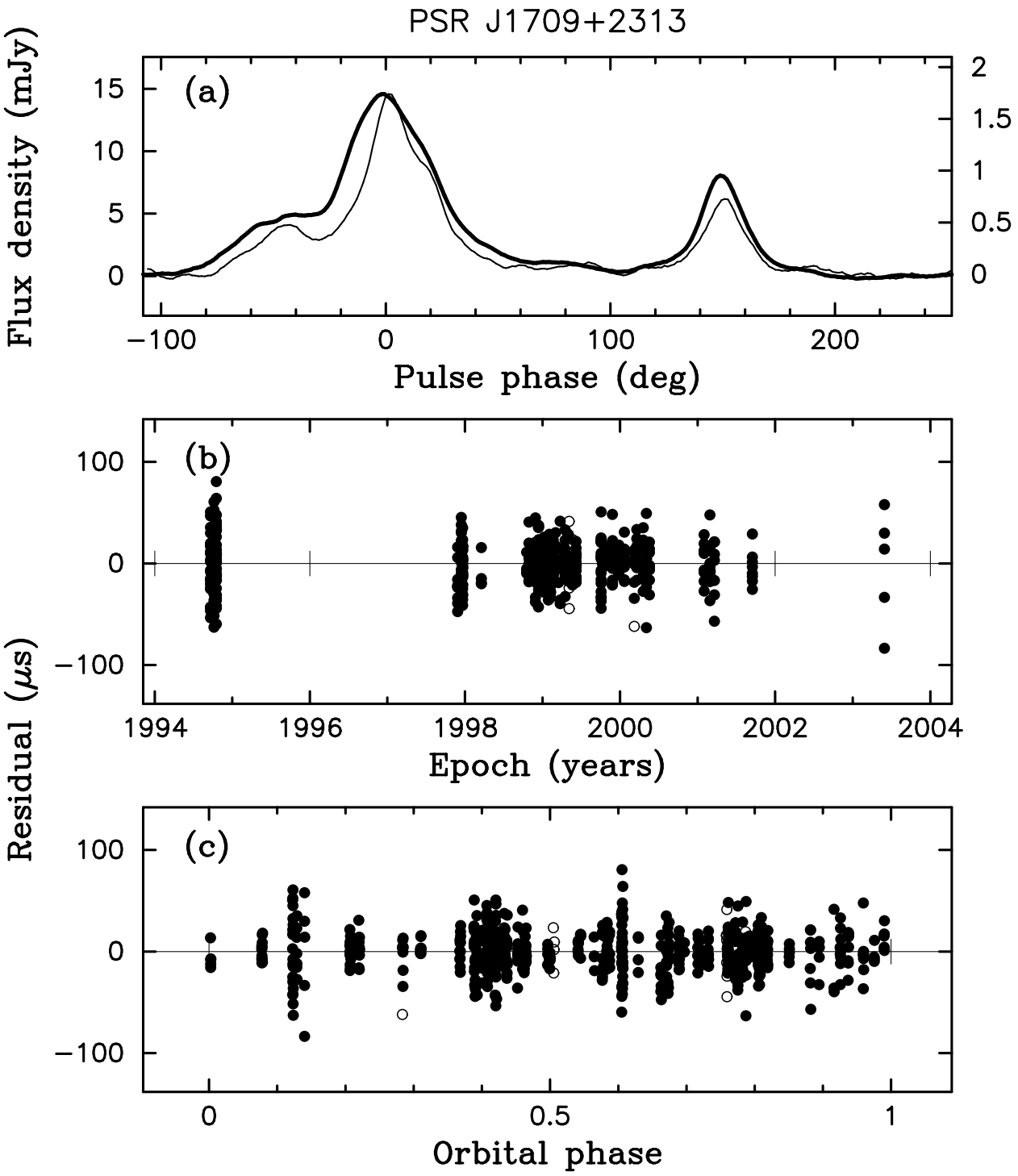

Fig. 1.— Observations of the 4.6-ms pulsar PSR J1709+2313 with the Arecibo telescope. (a) Average pulse profiles at 430 MHz (heavy solid line) and 1400 MHz (solid line). (b) The best-fit timing residuals as a function of time at 430 MHz (filled circles) and 1400 MHz (open circles). (c) Residuals as in (b) plotted against the orbital phase.

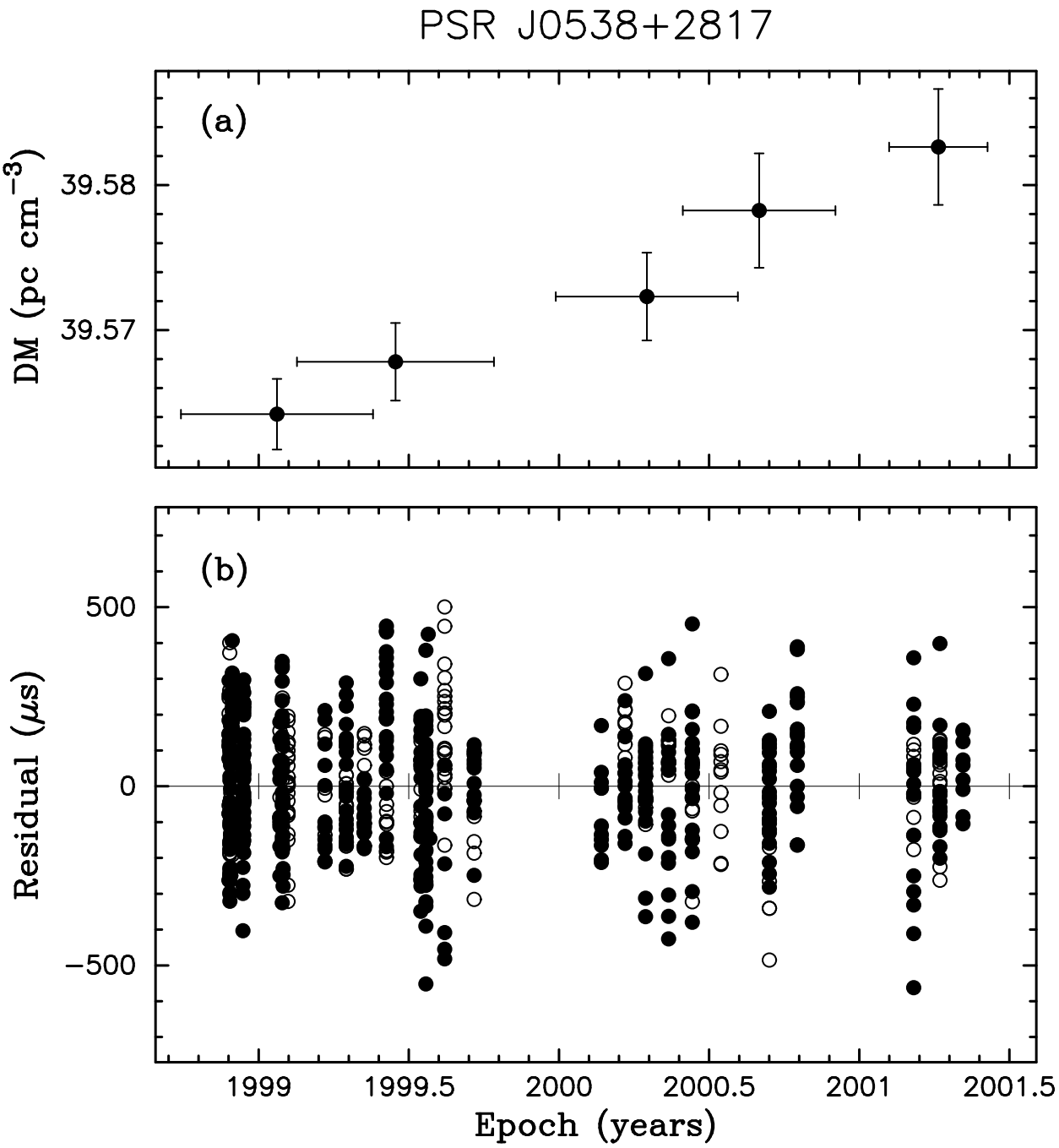

Fig. 2.— Arecibo observations of PSR J0538+2817 in the supernova remnant S147. (a) Dispersion measure variations over the observing period (see text for details). (b) The best-fit timing residuals at 430 MHz (filled circles) and 1400 MHz (open circles).

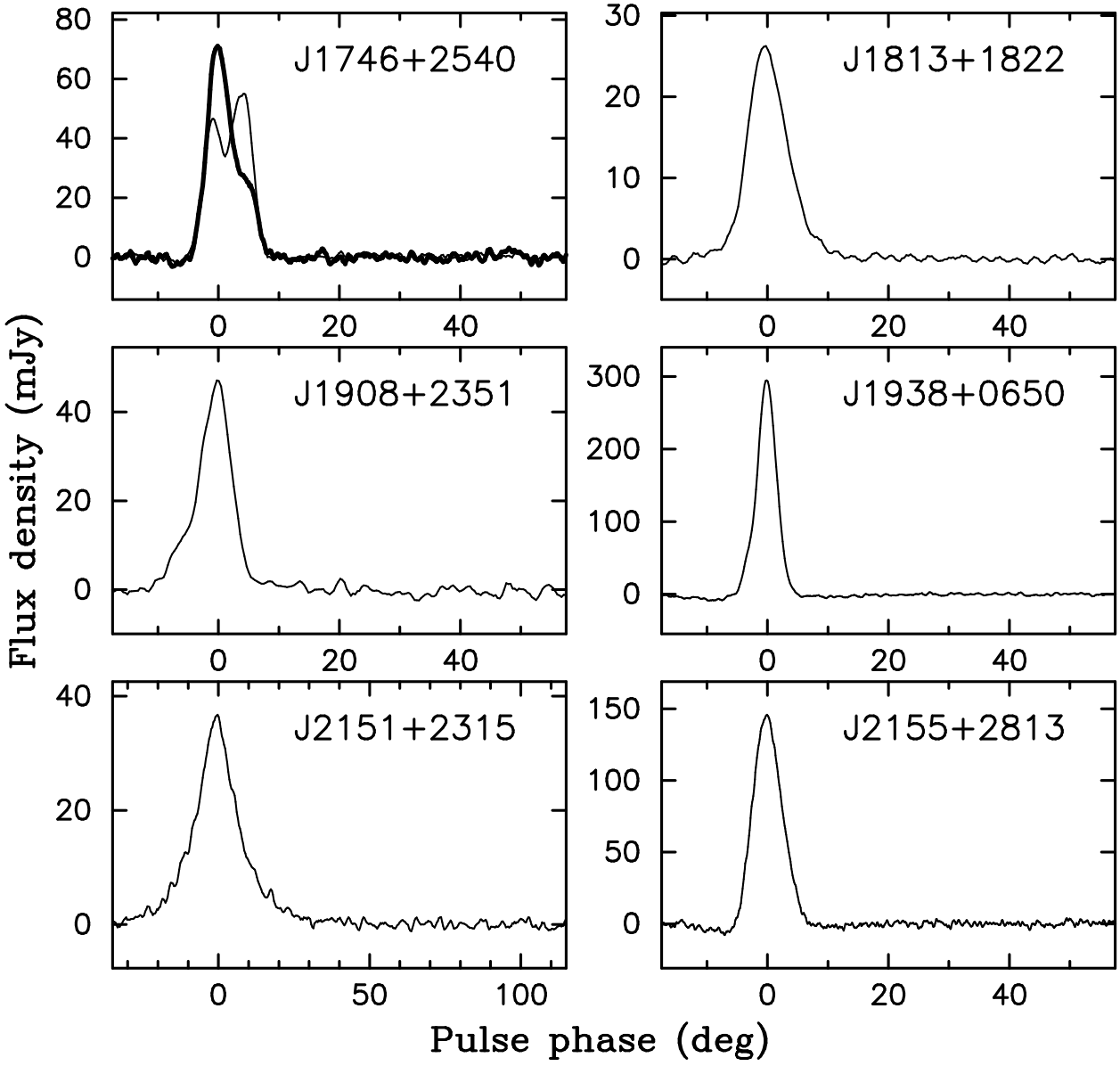

Fig. 3.— Previously unpublished average pulse profiles at 430 MHz. For the mode-changing pulsar PSR J1746+2540, two stable profile modes are displayed.

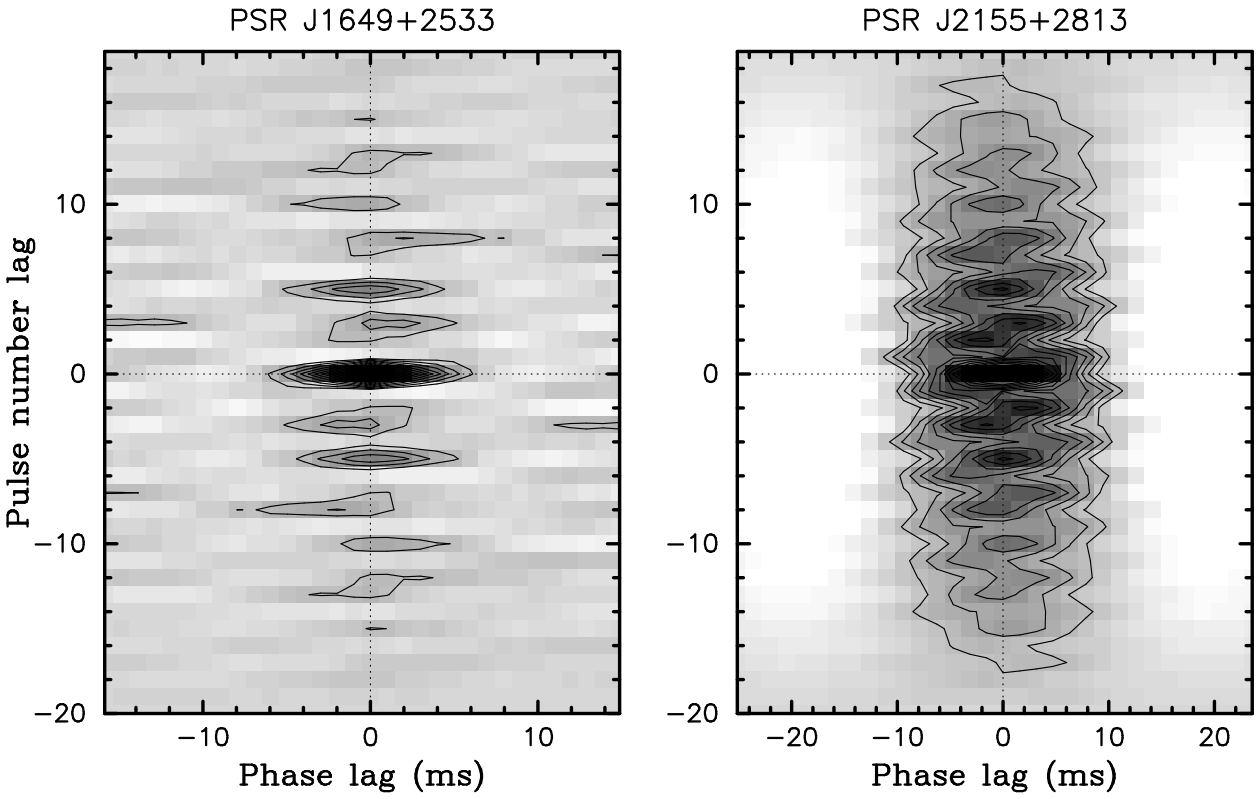

Fig. 4.— Normalized, two-dimensional autocorrelation functions of single pulse sequences from PSR J1649+2533 and PSR J2155+2813 at 430 MHz. The correlation coefficient is mapped in the range of 0.05 to 0.95 at the contour interval of 0.05.

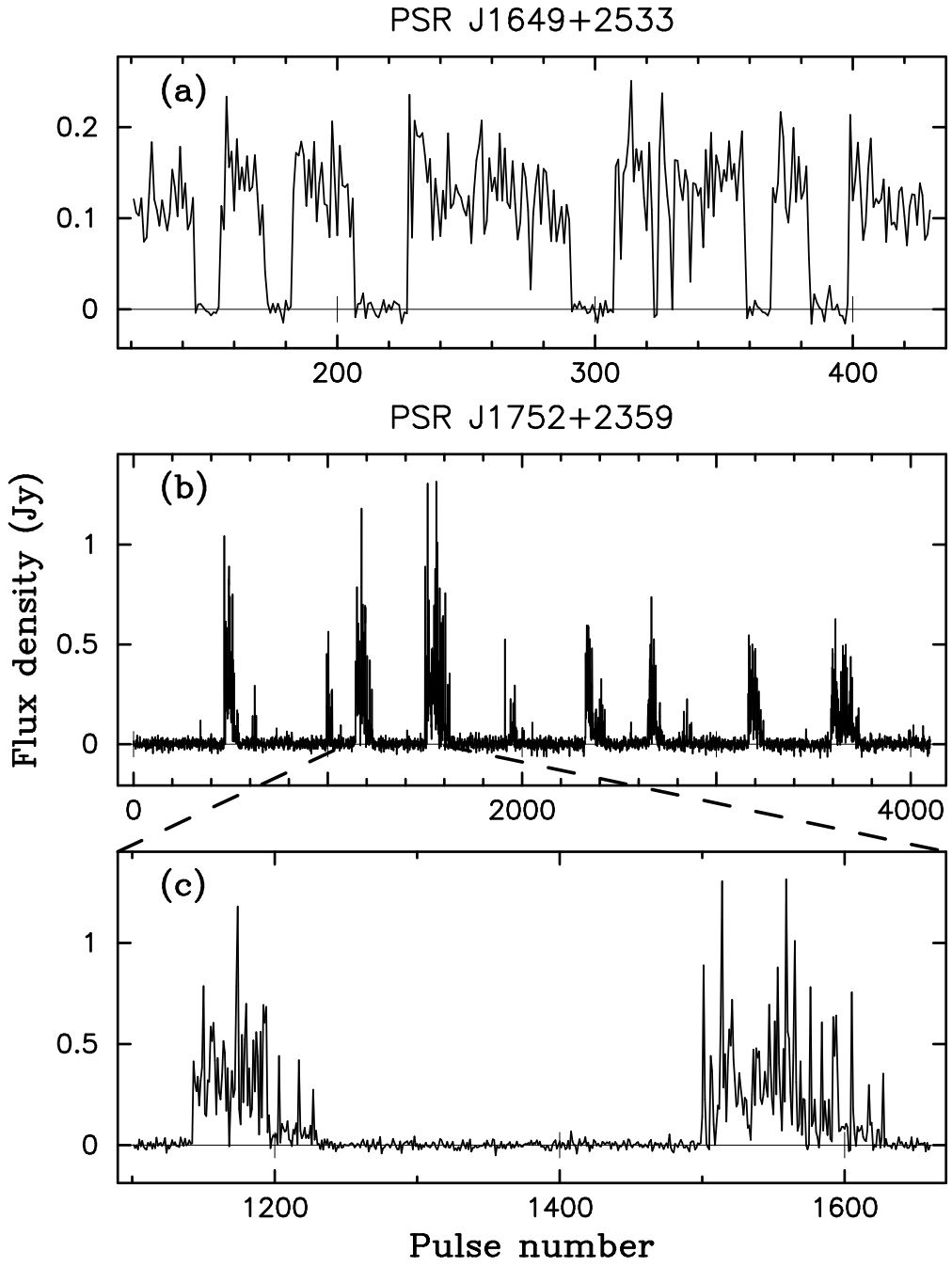

Fig. 5.— Pulse-to-pulse intensity variations in PSR J1649+2533 and PSR J1752+2359 at 430 MHz. (a) Pulse nulling in PSR J1649+2533. (b) An example of the bursting behavior of PSR J1752+2359. (c) Details of the intensity variations in two consecutive bursts.

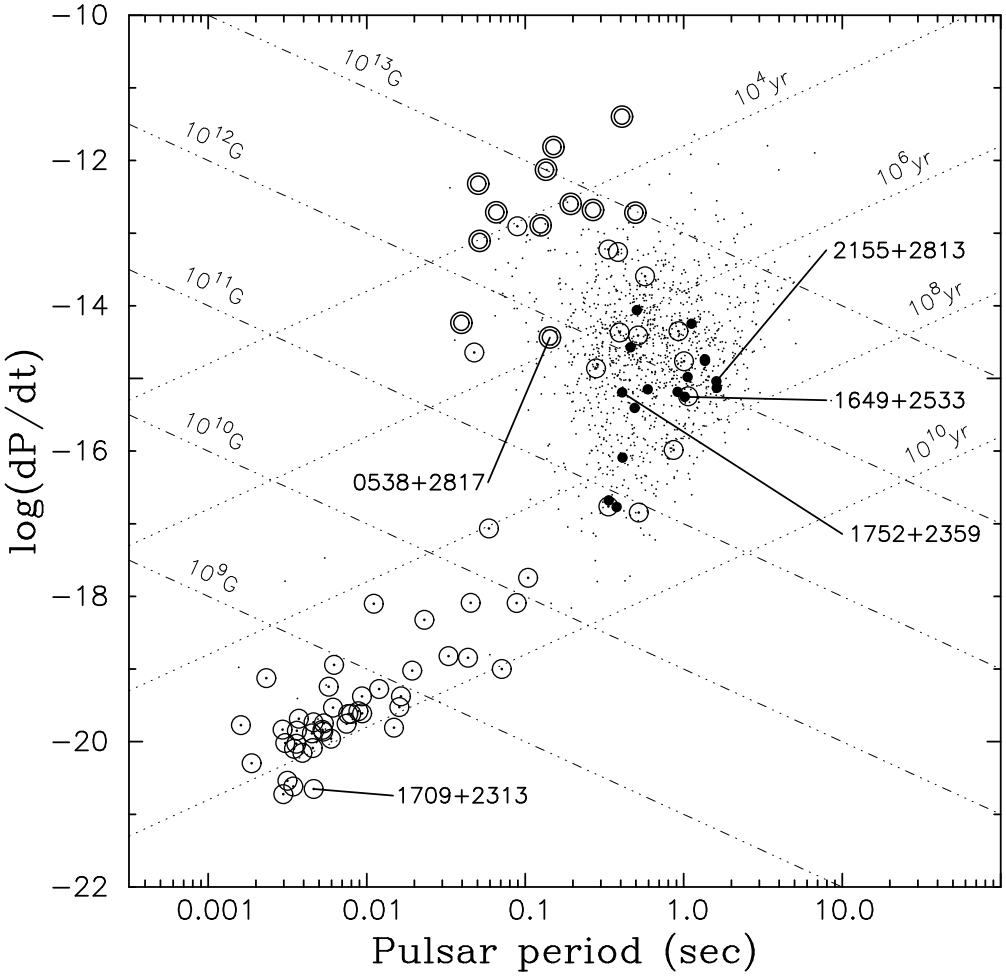

Fig. 6.— Distribution of the 18 pulsars discussed in the text in the P-$\dot{P}$ diagram based on the ATNF pulsar catalog (`http://www.atnf.csiro.au/research/pulsar/catalogue`). Individually discussed objects are indicated by names. The other new pulsars are denoted by filled circles. The catalog data used include isolated pulsars (dots), binary pulsars (encircled dots) and pulsars associated with supernova remnants (double circles). Lines of constant magnetic field and age are drawn with the dash-dotted and dotted lines, respectively.

Table 1. Parameters for PSR J1709+2313.

Parameter	Value
Right ascension α (J2000)	$17^h09^m05\overset{s}{.}792(6)$
Declination δ (J2000)	$23^o13'27\overset{''}{.}85(1)$
Proper motion μ_α (mas yr^{-1})	$-3.2(7)$
Proper motion μ_δ (mas yr^{-1})	$-9.7(9)$
Spin frequency ν (s^{-1})	215.926931187247(7)
First derivative $\dot{\nu}$ ($\times 10^{-15}$ s^{-2})	$-0.1692(2)$
Spin period P (s)	0.004631962778409(2)
Period derivative $\dot{P}$ ($\times 10^{-15}$)	0.00000363(4)
Kinematic correction $\dot{P}_k$ ($\times 10^{-15}$) ...	0.0000014(4)
Position and frequency epoch (MJD) .	51145.0
Dispersion Measure DM (pc cm^{-3}) ..	25.3474(2)
Orbital period P_b (days)	22.71189238(2)
Projected semi-major axis $a \sin i$ (lt-s)	15.288544(2)
Eccentricity e	0.0000187(2)
Time of periastron passage T_p (MJD)[a]	51196.24079 ± 0.036
Longitude of periastron ω (deg)[a].....	$24\overset{\circ}{.}30300 \pm 0.58$
Minimum companion mass $m_c(M_\odot)$ ..	0.27
Tranverse velocity v_t (km/s)	89(30)[b]
Pulse width at FWHM, w_{50} (ms)[c]	0.52 / 0.34
Pulse width at 10% peak, w_{10} (ms)[c] ..	1.31 / 1.14
Equivalent width, w_e (ms)[c]	0.58 / 0.50
Average flux (mJy)[c]	2.52(7) / 0.2(1)

[a] as the precission of T_p and ω is too low for observational purposes, we quote extra digits for the benefit of future observers

[b] error includes contribution from uncertainty in distance estimate

[c] values at 430/1400 MHz

Table 2. Astrometric, spin and derived parameters for PSR J0538+2817.

Parameter	Value
Ecliptic longlitude λ	$85\overset{\circ}{.}232546(1)$
Ecliptic latitude β	$4\overset{\circ}{.}93582(3)$
Proper motion μ_λ (mas yr^{-1})	$-27(6)$
Proper motion μ_β (mas yr^{-1})	129(118)
Right ascension α (J2000)[a].....	$5^h38^m25\overset{s}{.}06$
Declination δ (J2000)[a].....	$28^o17'09\overset{''}{.}10$
Spin frequency ν (s^{-1})	6.985269943305(6)
First derivative $\dot{\nu}$ ($\times 10^{-15}$ s^{-2})	$-179.0720(6)$
Spin period P (s)	0.143158390172(1)
Period derivative $\dot{P}$ ($\times 10^{-15}$)	3.6699(1)
Position and frequency epoch (MJD)	51500.0
Dispersion Measure DM (pc cm^{-3})[b].	39.569
Pulse width at FWHM, w_{50} (ms)[c]...	4.1 / 2.7
Pulse width at 10% peak, w_{10} (ms)[c].	17.8 / 13.9
Equivalent width, w_e (ms)[c].....	7.6 / 5.9
Average flux (mJy)[c].....	8.2(2) / 1.9(1)

[a] calculated from the best-fit ecliptic coordinates

[b] see text and Fig. 2 for data on DM variability

[c] values at 430/1400 MHz

Table 3: Parameters for 16 slow pulsars.

PSR	R. A. (J2000)	Dec (J2000)	P (s)	$\dot{P}$ (10^{-15})	Epoch (MJD)	DM (pc/cm^3)	w_e (ms)	w_{50} (ms)	w_{10} (ms)	S_{430} (mJy)
J1627+1419	16:27:18.77(1)	14:19:20.5(3)	0.4908568275(6)	0.3931(1)	51825.0	33.8(6)	28	30	41	6.1(3)
J1645+1012	16:45:34.4(2)	10:12:16.0(4)	0.410860739492(2)	0.0812(5)	51825.0	36.3(6)	11	11	19	2.3(1)
J1649+2533	16:49:44.23(5)	25:33:07.0(2)	1.0152573918(5)	0.5594(2)	51825.0	35.5(9)	24	25.	38	7.4(4)
J1652+2651[a]	16:52:03.07(3)	26:51:40.4(4)	0.91580349720(5)	0.6537(1)	51739.0	41.2(3)	24	12,14	43	11.3(1)
J1720+2150[a]	17:20:01.30 (2)	21:50:12.8(4)	1.61566378034(7)	0.740(2)	51796.0	41.1(4)	25	8,7	70	2.4(1)
J1741+2758[b]	17:41:53.51(2)	27:58:09.0(9)	1.3607376877(4)	1.841(1)	51797.0	29.3(6)	18	7,4	40	3.0(1)
J1746+2540[A]	17:46:06.87(6)	25:40:37.5(1)	1.0581481703(1)	1.047(2)	51796.0	51.5(2)	21	24	33	1.2(1)
J1746+2540[B]							17	13	31	
J1752+2359	17:52:35.42(2)	23:59:48.2(2)	0.409050865044(9)	0.6427(9)	51952.0	36.0(9)	5	4	11	3.5(3)
J1811+0702[c]	18:11:20.42(7)	07:02:29.7(2)	0.46171267661(3)	2.692(1)	51885.0	57.8(1)	17	−,13	15,21	2.2(1)
J1813+1822	18:13:38.76(5)	18:22:15.0(9)	0.3364246764(9)	0.021(8)	51886.0	60.8(5)	8	6	13	0.6(1)
J1822+0705 [d]	18:22:18.44(2)	07:05:20.1(1)	1.3628174508(2)	1.749(5)	51730.0	61.2(5)	21	9,10	40,19	3.8(1)
J1848+0647	18:48:56.01(3)	06:47:31.7(4)	0.5059567391(2)	8.7516(1)	51824.0	27.9(2)	14	15	27	2.3(1)
J1908+2351	19:08:31.94(7)	23:51:41.9(8)	0.377578026(1)	0.017(1)	51561.0	101.5(7)	7	6	14	0.9(2)
J1938+0650	19:37:53.46(4)	06:50:06.0(2)	1.121561892(5)	5.68(1)	51824.0	70.8(2)	12	10	22	3.2(1)
J2151+2315	21:51:28.9(1)	23:15:12.8(5)	0.593533613(3)	0.708(3)	51594.0	23.6(2)	30	23	68	1.6(1)
J2155+2813	21:55:15.82(1)	28:13:12.1(2)	1.6090199964(6)	0.9164(9)	51594.0	77.4(2)	25	24	42	2.1(1)

[A,B] modes of PSR J1746+2540

[a] double profile with "bridge"

[b] blended multiple component profile, two components rise above 50% of maximum height

[c] two separate components, left one does not reach 50% of maximum height

[d] two separate components

Table 4: Derived parameters for 18 pulsars.

Pulsar	d(kpc)	z(kpc)	log [L_{430} (mJy kpc^2)]	τ(Myr)	log[$\dot{E}$ (ergs s^{-1})]	log [$B(G)$]
J0538+2817.....	1.78	0.052	3.23	0.62	34.7	11.9
J1627+1419.....	>2.84	>1.76	1.7	19.7	32.1	11.6
J1645+1012.....	>3.27	>1.75	1.3	80.1	31.6	11.2
J1649+2533.....	>2.91	>1.75	1.8	28.7	31.3	11.9
J1652+2651.....	>2.93	>1.76	2.0	22.2	31.5	11.9
J1709+2313.....	1.83	0.97	2.13	33300	32.4	8.01
J1720+2150.....	>3.59	>1.76	1.5	34.6	30.8	12.0
J1741+2758.....	2.07	0.93	0.6	11.7	31.4	12.2
J1746+2540.....	>4.16	>1.76	1.3	16.0	31.5	12.0
J1752+2359.....	2.70	1.05	1.4	10.1	32.6	11.7
J1811+0702.....	3.13	0.65	1.3	2.7	33.0	12.0
J1813+1822.....	>6.24	>1.76	1.4	253.8	31.3	10.9
J1822+0705.....	2.98	0.50	1.5	12.3	31.4	12.2
J1848+0647.....	1.44	0.09	0.7	0.9	31.4	12.3
J1908+2351.....	6.62	0.81	1.6	358.8	31.1	10.9
J1938+0650.....	3.64	−0.45	1.6	3.1	32.2	12.4
J2151+2315.....	1.42	−0.57	0.5	13.2	32.1	11.8
J2155+2813.....	>5.06	< -1.76	1.73	27.8	30.9	12.1